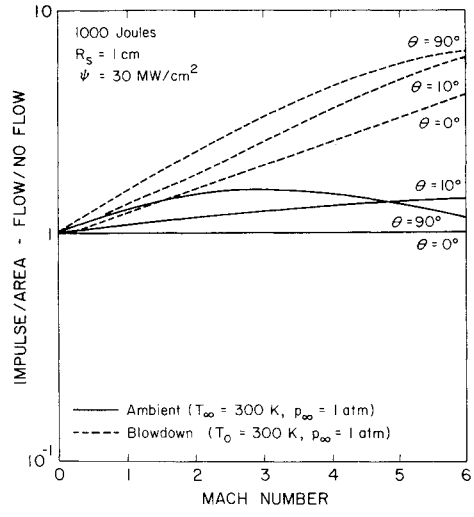

Fig. 3 Impulse/area.

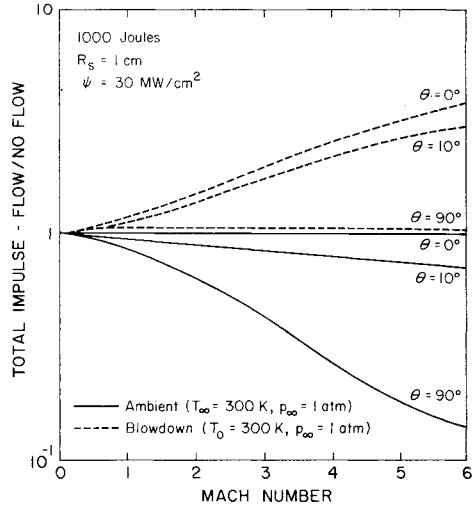

Fig. 4 Total impulse

blowdown simulation will create an artifact due to the higher densities and lower temperatures. The model predictions for total impulse are illustrated in Fig. 4. Again, the blowdown simulation yields enhancement, whereas the real atmosphere does not. The serious degradation of the impulse for $\theta = 90$ deg is due to the extremely high temperatures behind the normal shock wave. The hotter gas simply expands faster and imparts less impulse than a cold gas at the same pressure.

Conclusions

An assessment has been made of the effect of supersonic flow on the impulse imparted to a surface by laser irradiation. Near-field enhancement is dependent on the dynamic pressure of the gas, whereas the far-field enhancement is a function of whether one is concerned with the impulse or the impulse per unit area, blowdown simulation or the real atmosphere, and which flow regime is encountered.

Near-field enhancement in the atmosphere is relatively insignificant and occurs only at low values of p_s (of the order of p_0). Far-field enhancement in the atmosphere can be either positive or negative. For the cases considered, variations in the impulse per unit area are not dramatic, but a serious degradation in the total impulse can occur at high Mach numbers. This is due to the high gas temperature. The thermal velocity of the gas is so large that the gas escapes the surface in a relatively short time and prevents a significant impulse from being imparted.

Simulation of the flow environment is necessary in order to conduct laser-induced impulse measurements. An unheated blowdown facility matches the dynamic and static pressures, thereby simulating the near-field effect, but does not match the total temperature ($T_0 = 300$ K). The gas in the tunnel is then colder and denser than in the real atmosphere at the same pressure and Mach number ($\rho, T,$ and u are not matched). The scaling laws in Table 1 indicate that a greater impulse will occur in the blowdown facility than in the real atmosphere. Hence, the unheated blowdown test facility is inadequate for examining the "enhancement" of laser-induced impulse with supersonic flow.

Acknowledgment

This research was supported by the Naval Research Laboratory, Contract N00014-83-C-2255, monitored by Dr. Clarence Bond.

References

[1]Woodroffe, J. A., Stankevics, J. O. A., Ballantyne, A., and Reilly, J. P., "Pulsed Laser-Generated Impulse on a Surface in Supersonic Flow," *AIAA Journal,* Vol. 18, Jan. 1980, pp. 94-95.

[2]Reilly, J. P., Ballantyne, A., and Woodroffe, J. A., "Modeling of Momentum Transfer to a Surface by Laser Supported Absorption Waves," *AIAA Journal,* Vol. 17, Oct. 1979, pp. 1098-1105.

[3]Pirri, A. N., "Theory for Momentum Transfer to a Surface with a High Power Laser," *Physics of Fluids,* Vol. 16, Sept. 1973, pp. 1435-1440.

[4]Simons, G. A., "Asymptotic Theory for the Momentum Transfer to a Surface when Irradiated by a High Power Laser," *AIAA Journal,* Vol. 22, Sept. 1984, pp. 1275-1280.

Pulsed DF Laser/Metal Interaction in Direct Absorption Regime

Peter K. S. Wu,* Robert G. Root,† and Anthony N. Pirri‡
Physical Sciences Inc., Andover, Massachusetts
and
Michael F. Weisbach§
Boeing Aerospace Company, Seattle, Washington

Introduction

THE phenomenology associated with high-power laser irradiation of metals has been extensively studied,[1-4] primarily in the context of 10.6 μm laser radiation. In this Note, the theoretical models are modified to describe the interaction of DF laser radiation with metals and predict an important quantity, the "residual energy," defined as that portion of pulse energy remaining in the target after the termination of the laser pulse. The accumulation of residual energy in a repetitively pulsed interaction is expected to heat the bulk sample to the solidus temperature where the target fails.

The mechanisms by which the coupling is achieved are markedly different between 10.6 and 3.8 μm interactions. The pulsed 10.6 μm laser/metal interaction is controlled by the gain-switched spike that occurs at the beginning of the laser

Received April 13, 1984; revision received Oct. 29, 1984.

*Principal Research Scientist. Member AIAA.
†Director, Applied Sciences; presently with Sparta, Lexington, Mass.
‡Vice President, Defense Programs.
§Senior Engineer.

pulse and comprises only a small portion of the total pulse energy. The thermal coupling of pulsed 10.6 μm radiation to metals depends upon both the size of the leading-edge gain-switched spike, which is responsible for plasma ignition, and the average laser intensity, which determines the properties of the plasma (if present). The DF laser pulse does not have a leading-edge spike. Rather, it exhibits a relatively long rise time of approximately 1 μs, which does not ignite a plasma at the leading edge. For typical experiments[5,6] with pulsed 3.8 μm laser radiation, plasma initiation occurs in the middle of the laser pulse. Hence, the contribution from direct absorption of the laser radiation must always be included in the coupling calculations even for pulse fluence greater than the plasma ignition threshold. The direct absorption of laser radiation cannot be simply characterized by the intrinsic room temperature absorptivity as it can for 10.6 μm. In addition, for existing high-power pulsed DF laser systems at TRW and Boeing, the absorbed heat flux is more than an order of magnitude higher than those for the AVCO 10.6 μm laser because of higher peak intensity and higher absorptivity.

This Note addresses the response of Al2024, Al1100, and multiple-pulse roughened Al2024 targets to pulsed DF laser radiation in the direct absorption regime, which is the first part of a potentially two-part issue. The complex phenomenology of pulsed laser/metal interaction in the plasma regime has been examined in Ref. 7.

Analysis

A one-dimensional transient heat conduction problem has been formulated for laser/metal interaction. The governing equation can be written as

$$\rho c_p(T)\frac{\partial T}{\partial t}=\frac{\partial}{\partial x}\left[k(T)\frac{\partial T}{\partial x}\right] \tag{1}$$

where x is the distance, t the time, T the temperature, ρ the density, c_p the specific heat, and K the thermal conductivity. Equation (1) has been solved by an explicit forward-marching technique in finite difference form with the initial condition $T(x,t=0)=T_0(x)$ and the boundary conditions for $t>0$

$$-K\frac{\partial T}{\partial x}\bigg|_{x=0}=\alpha(T_s)I(t)-\dot{m}H_v-\epsilon\sigma T_s^4 \tag{2}$$

where $I(t)$ is the incident laser intensity; $\alpha(T_s)$ the target absorptivity, which is a function of the surface temperature T_s; $\dot{m}$ the mass vaporization rate; H_v the latent heat of vaporization; ϵ the target emissivity; and σ the Stephan-Boltzmann constant.

For 10.6 μm radiation, the breakdown process has been analyzed in detail by Weyl et al.,[8] who shows that the defects must first vaporize before breakdown occurs in the hot high-pressure vapor. The prompt ignition model has been extended to 3.8 μm radiation with the vapor provided by the bulk surface vaporization instead of the breakdown of defects.[9] The theoretical prediction of ignition time agrees well with the experimental data.[7] Here, two simplistic limits are presented for reference for pulse fluence greater than the plasma ignition threshold.

For 3.8 μm radiation, the room temperature intrinsic absorptivity of Al2024 has been measured by Schriempf[10] to be about 0.05 (0.03 for 10.6 μm radiation). For the low-temperature range, i.e., less than the solidus temperature of 775 K, the absorptivity is assumed to be linear, as derived by Touloukian.[11] The absorptivity rises from about 0.05 at 300 K to 0.08 at 775 K. Robin and Nordin[12] have measured the absorptivity to be about 0.14 at the liquidus temperature (911 K) to 0.18 at 1400 K. Since the phase change does not take place until the temperature reaches the liquidus[13] a linear extension is used between the solidus and the liquidus temperatures. A linear extension is also used for temperatures greater than about 1400 K.

For Al1100, the room temperature absorptivity has been taken to be that of pure aluminum ($\alpha=0.03$).[11] For the low-temperature range (less than liquidus temperature 930 K), the slope of the absorptivity curves for Al1100 and Al2024 are the same and at higher temperature (>930 K) the absorptivity for Al1100 is identical to that of Al2024.

In formulating this model, it is assumed that the entire heat of fusion is provided at the liquidus temperature and that the surface mass loss rate is adequately approximated by

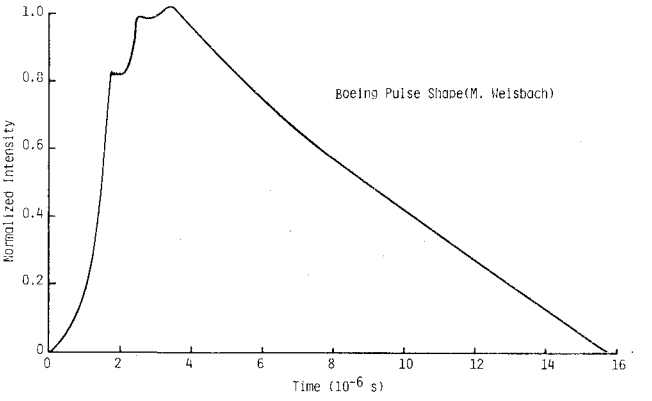

Fig. 1 Incident pulse intensity temporal profile.

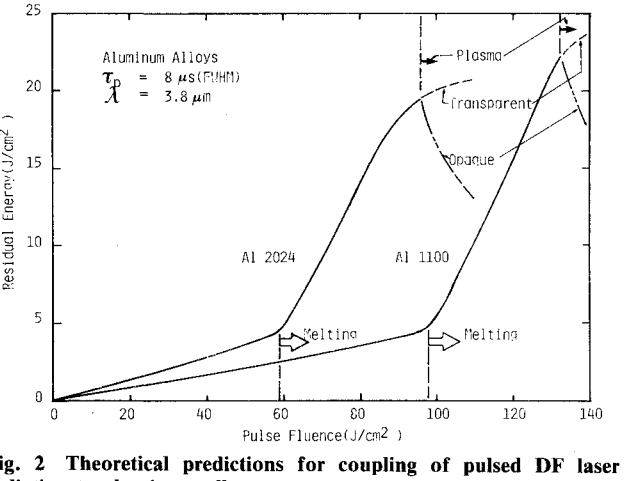

Fig. 2 Theoretical predictions for coupling of pulsed DF laser radiation to aluminum alloys.

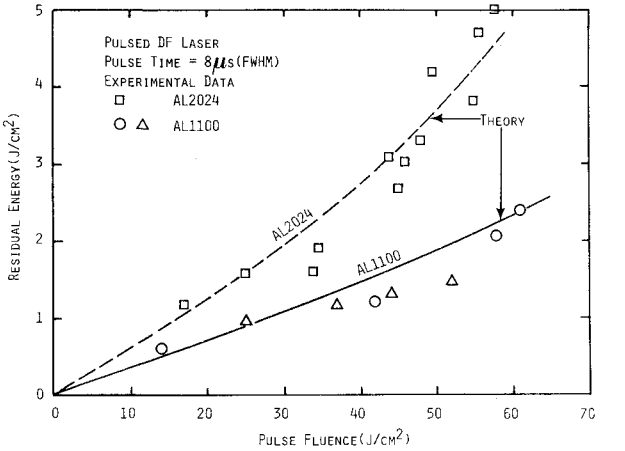

Fig. 3 Theory/data comparison for pulsed DF laser interactions with Al2024 and Al1100 targets.

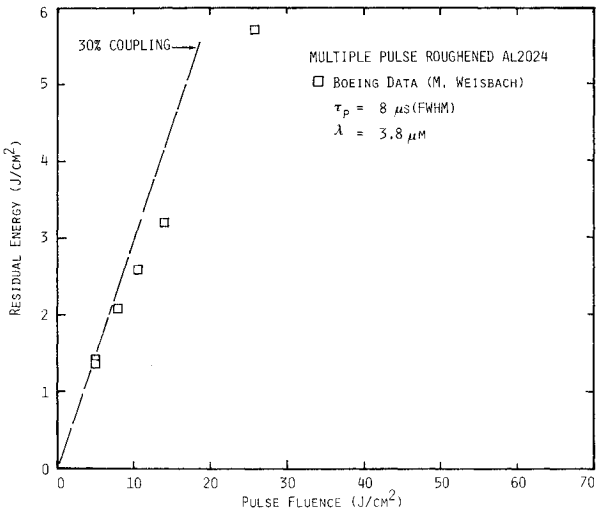

Fig. 4 Experimental measurements of residual energy as a function of pulse fluence (multiple-pulse roughened Al2024).

the analysis of Knight.[14] For Al2024, the thermal conductivity and the heat capacity of Al2024 are obtained from Refs. 11 and 15. For Al1100, which is considered to be pure aluminum, the specific heat is obtained from Ref. 16, while thermal diffusivity is given in Ref. 17. With the temperature-dependent absorptivity and the thermophysical properties of Al2024 and Al1100 well defined, one can readily calculate the residual energy in the interaction of pulsed 3.8 μm laser radiation with aluminum targets.

Experimental Conditions

Experiments have been conducted on targets of 2024 and 1100 aluminum. In these experiments, a pulsed DF laser beam of approximately 310 J, having a pulse width of 8 μs and an initial rise time of 3 μs, is incident on the target. The spot size is varied over a range of about 5-50 cm^2 by the positioning of the target in the focused beam, in order to vary the incident intensity. The intensity on the target is uniform to within about 20% over the illuminated area and is kept sufficiently low so that in no case is a plasma formed on the target surface.

The absorbed fluence (residual energy) is deduced from the temperature (measured with a thin-wire thermocouple) at the center of the back surface of the large (compared to the laser spot), thin (0.050 in.) target, utilizing the analysis developed by Hall.[18]

Results and Discussion

Coupling calculations have been carried out for the interactions of 3.8 μm laser radiation with experimentally measured pulse shape (Fig. 1) with Al2024 and Al1100 targets. The radiation and ablation losses are, in general, small. For example, consider pulse fluence of 87 J/cm^2 (just below the plasma ignition threshold) and an Al2024 target. The radiation loss is about 10^{-3} J/cm^2 and the ablation loss is approximately 0.8 μm. The results of residual energy are given in Fig. 2. The theoretical predictions have been provided for pulse fluences up to plasma ignition thresholds. In the plasma regime, results show two limits where the vapor is either transparent or opaque to the plasma reradiation. As shown in Fig. 2, the residual energy in the direct absorption regime consists of two distinct regions of initial low absorption and of melt. The transition occurs at the pulse fluence where the maximum surface temperature reaches the liquidus temperature and the residual energy rises sharply with further increase in pulse fluence to as high as about 20 J/cm^2.

The experimental data have been taken primarily in the initial low-absorption region. The results of experiments with "as-received" (from the manufacturer) targets of Al2024 and Al1100 are shown in Fig. 3, in which the calculations compare favorably with the data. The coupling of 3.8 μm laser radiation to Al1100 target is expected to be lower than that for Al2024 target because of the lower absorptivity and higher thermal conductivity of Al1100. For the multiple-pulse roughened Al2024 interaction experiment, one of the samples was measured with a spectrophotometer, indicating a reflectance of 70% at 3.8 μm (in this respect, the material is not unlike grit-blasted aluminum).[11] The results of the experiments are shown in Fig. 4. The low fluence measurements confirm the reflectance measurement and, at higher fluence, it appears that the absorptivity actually decreases somewhat. The coupling enhancement due to multiple-pulse effects, which cannot be explained by the one-dimensional model, requires further study because of its application in the repetitively pulsed DF laser interaction with aluminum targets.

Acknowledgment

This work was sponsored by the Naval Research Laboratory under Contract 00014-82-C-2486, NRL Project Manager, Stuart K. Searles.

References

[1]Pirri, A. N., Kemp, N. H., Root, R. G., and Wu, P.K.S., "Theoretical Laser Effects Studies—Final Report," Physical Sciences Inc., Andover, MA, Rept. TR-89, Feb. 1977.

[2]Pirri, A. N, Root, R. G., and Wu, P.K.S., "Analytical Laser/Material Interaction Investigations," Vols. I and II, Physical Sciences Inc., Andover, MA, Rept. TR-104, Sept. 1977.

[3]Boni, A. A., Su, F. Y., Thomas, P. D., Musal, H. M., "Theoretical Study of Laser-Target Interactions," Science Applications Inc., LaJolla, CA, Final Tech. Rept. SAI 77-567 LJ, May 1977.

[4]Pirri, A. N., Root, R. G., and Wu, P.K.S., "Plasma Energy Transfer to Metal Surfaces Irradiated by Pulsed Lasers," *AIAA Journal*, Vol. 16, Dec. 1978, pp. 1296-1304.

[5]Maher, W. E., Nichols, D. B., and Hall, R. B., "Multiple-pulse Thermal Coupling at 3.8 μm Wavelength," *Applied Physics Letters*, Vol. 37, Jan. 1980, pp. 12-14.

[6]Holmes, B. S., Maher, W. E., and Hall, R. B., "Laser-target Interaction Near the Plasma-Formation Threshold," *Journal of Applied Physics*, Vol. 51, Nov. 1980.

[7]Wu, P.K.S., Root, R. G., and Pirri, A. N., "Effects of Apor Layer on the Coupling of Pulsed DF Laser Radiation to Al 2024," AIAA Paper 84-1783, June 1984.

[8]Weyl, G., Pirri, A., and Root, R. G., "Laser Ignition of Plasma Off Aluminum Surfaces," *AIAA Journal*, Vol. 19, 1980, p. 460.

[9]Root, R. G., Wu, P.K.S., Popper, L. A., Hastings, D. E., Clarke, A. S., and Pugh, E. R., "Repetitively Pulsed Laser Effects Studies," U.S. Army Missile Command, Tech. Rept. RH-CR-82-17, April 1982.

[10]Schriempf, T., private communication, Naval Research Laboratory, Washington, D.C.

[11]Touloukian, Y. S. and Ho, C. Y., "Thermal Radiative Properties" *Thermophysical Properties of Selected Aerospace Materials*, Pt. I, Purdue University, Lafayette, IN, 1976.

[12]Robin, J. E. and Nordin, P., "Spectral Absorptance at 3.8 μm Wavelength for Aluminum and Pyroceram at Elevated Temperatures," *Applied Physics Letters*, Vol. 27, No. 9, 1975, pp. 493-495.

[13]Holsapple, K. A. and Schmidt, R. M., "Theory and Experiments on Rapid Melting of Metals," *Journal of Applied Physics*, Vol. 49, Nov. 1978, pp. 5493-5501.

[14]Knight, C. J., "Theoretical Modeling of Rapid Surface Vaporization with Back-Pressure," AIAA Paper 78-1220, July 1978.

[15]Touloukian, Y. S. and Ho, C. Y., (eds.), "Thermophysical Properties of Seven Materials," *Thermophysical Properties of Selected Aerospace Materials*, Pt. II, Purdue University, West Lafayette, IN, 1975.

[16]Touloukian, Y.S. (eds.), "Elements," *Thermophysical Properties of High Temperature Solid Materials*, Vol. 1, Macmillan Co., NY, 1967, p. 11.
[17]Touloukian, Y. S., Powell, R. W., Ho, C. Y., and Nicolaou, M. C., *Thermal Diffusivity*, IFI/Plenum, NY, 1973, p. 2.
[18]Maher, W. E. and Hall, R. B., "Experimental Thermal Coupling of Laser Beams," *Journal of Applied Physics*, April 1978.

Effects of Electric Fields on the Blowoff Limits of a Methane-Air Flame

R. I. Noorani*
The University of Southwestern Louisiana
Lafayette, Louisiana
and
R. E. Holmes†
Texas A&M University, College Station, Texas

Introduction

THE influence of electric fields applied to flames on extinction limits and flame stability have been reported by a number of researchers.[1-5] It is extremely difficult to draw precise conclusions concerning the effects of an electric field on flames due to the variety of experimental conditions and procedures employed by the various investigators; however, evaluation of the data indicates an increase in flame stability.

The main objective of this Note is to present the experimental results of the application of an electric field to the blowoff limits of a premixed methane-air flame. Methane-air flame is presently in worldwide use and is likely to become more important in energy economies based on fossil fuels in the near future. If the imposition of an electric field on a methane-air flame results in an increase in the extinction limits of a burner where extinction would normally occur were no field applied, burners could be operated at substantially leaner conditions—resulting in a potential increase in fuel efficiency.

In the present investigation, all experiments are performed with and without electric fields. The electric field was produced by a high-voltage dc power supply. The results of the investigation indicate that, under suitable electrode configuration, electric fields can be used as a suitable technique in controlling the combustion process.

Apparatus and Procedures

Tests on blowoff limits were carried out on two different geometries. Figure 1 represents the first geometry, consisting of a burner (Veriflow blowpipe, model 3A), a Pyrex glass tube of 11 cm diam, and a copper mesh electrode. The Pyrex tube was placed over the burner port in order to maintain an undisturbed flame. The mesh electrode was put on the top of the glass tube. A longitudinal electric field was obtained by connecting the copper mesh to the positive terminal of the dc power supply and the burner tube to the ground terminal.

Methane (99.7% purity) and air were fed into the burner through flowmeters attached to the gas and air cylinders, the air being of breathing quality.

Received June 2, 1984; revision received Nov. 19, 1984.

*Assistant Professor, Department of Mechanical Engineering.
†Associate Professor, Department of Mechanical Engineering.

The flame was always ignited at low velocities (approximately 33 cm^3/s) with an alcohol burner. The field was then turned on and the methane and air flow rates increased simultaneously up to the total velocity at which the blowoff limits were to be determined. Blowoff points were obtained by maintaining a constant flow of either the methane or air, while varying the other flow until the flame left the burner port.

By decreasing the gas flow rates, the lower blowoff limits were obtained, with and without electric fields. The upper blowoff points could not be obtained by increasing the gas flow rates because the flame picked up more air from the open surroundings at higher rates. As a result, another set of lower blowoff limits were obtained by keeping the gas flow rate constant and increasing the airflow rate.

Figure 2 represents the configuration for the second geometry. A longitudinal electric field was obtained by placing an aluminum foil ring around the glass tube for one electrode and making the brass burner the other electrode. Following the procedures of the first geometry, lower blowoff limits were obtained, with and without electric fields.

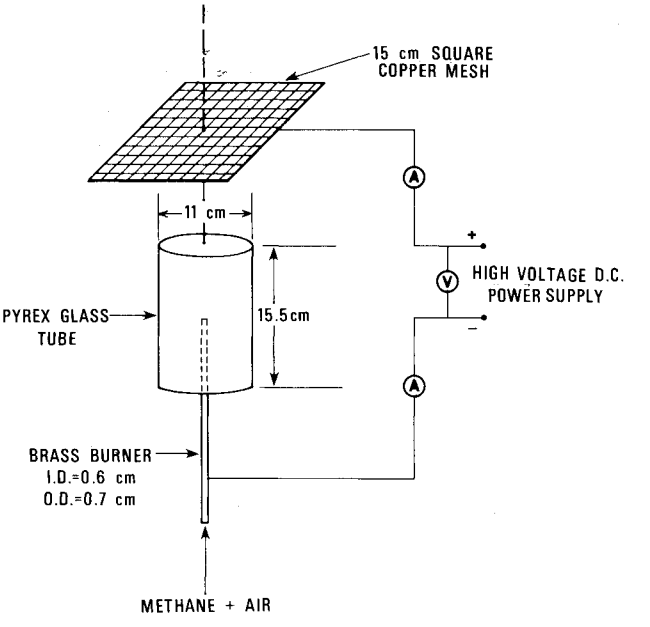

Fig. 1 Burner in longitudinal electric field with gage electrode.

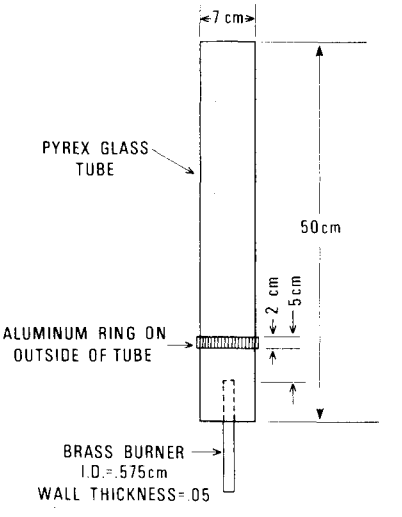

Fig. 2 Burner in longitudinal electric field.